

The CERN-ISOLDE fast tape station

S. Stegemann^{a,*}, D. Atanasov^a, M. Au^{a,b}, E. Grenier-Boley^a, M. Butcher^a, M. Duraffourg^a, E. Fadakis^a, T. Feniet^a, Y.N. Vila Gracia^a, T. Giles^a, J. Konki^a, L. Le^a, R. Lică^{a,c}, P. Martins^a, E. Matheson^a, C. Mihai^c, R. Martinez Muniz^a, C. Neacșu^{d,c}, G. Pascovici^c, K.A. Szczurek^a, S. Warren^a, S. Rothe^a

^a CERN, Geneva 23, 1211, Switzerland

^b Johannes Gutenberg-Universität, Mainz, 55122, Germany

^c H. Hulubei National Institute for Physics and Nuclear Engineering - IFIN-HH, Bucharest, R-077125, Romania

^d Physics Department, University "Politehnica" of Bucharest, Bucharest, R-060042, Romania

ARTICLE INFO

Keywords:

ISOLDE

Tape station

Radioactive ion beams

ABSTRACT

The employment of a suitable radioactive decay spectroscopy setup is essential for the operation of radioactive ion beam (RIB) facilities. CERN-ISOLDE recently developed a new fast tape station (FTS) setup to replace its more than 40 years old predecessor. The new FTS is equipped with several β -detectors, a HPGe-detector, provisions for an α -detector, and constitutes a significant improvement in terms of transport times and detector noise characteristics. Since 2021 it is routinely used as the primary asset for yield determination and quality control of produced RIBs at ISOLDE. We address in this work its technical features and introduce the utilized control system.

1. Introduction

CERN-ISOLDE is a research facility dedicated to the production of radioactive ion beams (RIBs) via the isotope separation on-line (ISOL) method [1]. Over the last 50 years more than 1000 isotopes have been produced from 76 different elements [2]. To enable smooth operation, ISOL facilities require an adequate radioactive decay detector setup. ISOLDE utilizes a tape station as a key component for the qualitative and quantitative analysis of produced RIBs. This includes production yield and beam purity measurements. In addition, the tape station is used as diagnostic tool during beam commissioning. The working principle is simple: produced RIBs are implanted onto a movable tape and transported to different detectors. Since the previous model served for more than 40 years, a new and improved tape station was recently commissioned. The new fast tape station (FTS) has a revised design, particularly in terms of tape speed, detector noise characteristics and reliability, which were considered the most striking shortcomings of the old version. First installed in 2016, commissioned in 2018 and moved during CERN's latest long shutdown to its final position in the ISOLDE experimental hall central beam line, the FTS completed its first two operational years during the ISOLDE physics campaigns in 2021 and 2022.

2. The new fast tape station at ISOLDE

2.1. Chassis

Detrimental timing and noise properties of the previous design prompted the development of the new and improved tape station. A picture taken close to its completion is shown in Fig. 1. The FTS is essentially a 2 m tall vacuum chamber, integrated into the ISOLDE central beam line. To achieve vacuum levels below 10^{-6} mBar, compatible to the beam line, the chassis comprises three machined chambers that are bolted together. Two chambers are the upper and lower tape boxes, containing two large tape reels, tension arms and a capstan that drives the rapid tape movement. The third chamber is the detector box, which will be explained in the next section. The aluminized Mylar tape (Goodfellow ES301955) is 50 μm thick, 12 mm wide and 1000 m long. Fast transport times (≈ 100 ms) are enabled by the 120 mm diameter and polyurethane-coated capstan, driven by a Siemens SIMOTICS S synchronous servo motor (1FK7032-5AK71-1DG5, 1.1 Nm, 0.5 kW). Tension arms located in both tape boxes allow rapid tape movement without the necessity to accelerate the large and heavy tape reels. In idle phase, i.e. in-between two measurement cycles, constant tension of the tape is guaranteed by two springs attached to each tension arm.

* Corresponding author.

E-mail address: simon.thomas.stegemann@cern.ch (S. Stegemann).

<https://doi.org/10.1016/j.nimb.2023.04.018>

Received 3 February 2023; Accepted 14 April 2023

Available online 23 May 2023

0168-583X/© 2023 The Authors. Published by Elsevier B.V. This is an open access article under the CC BY license (<http://creativecommons.org/licenses/by/4.0/>).

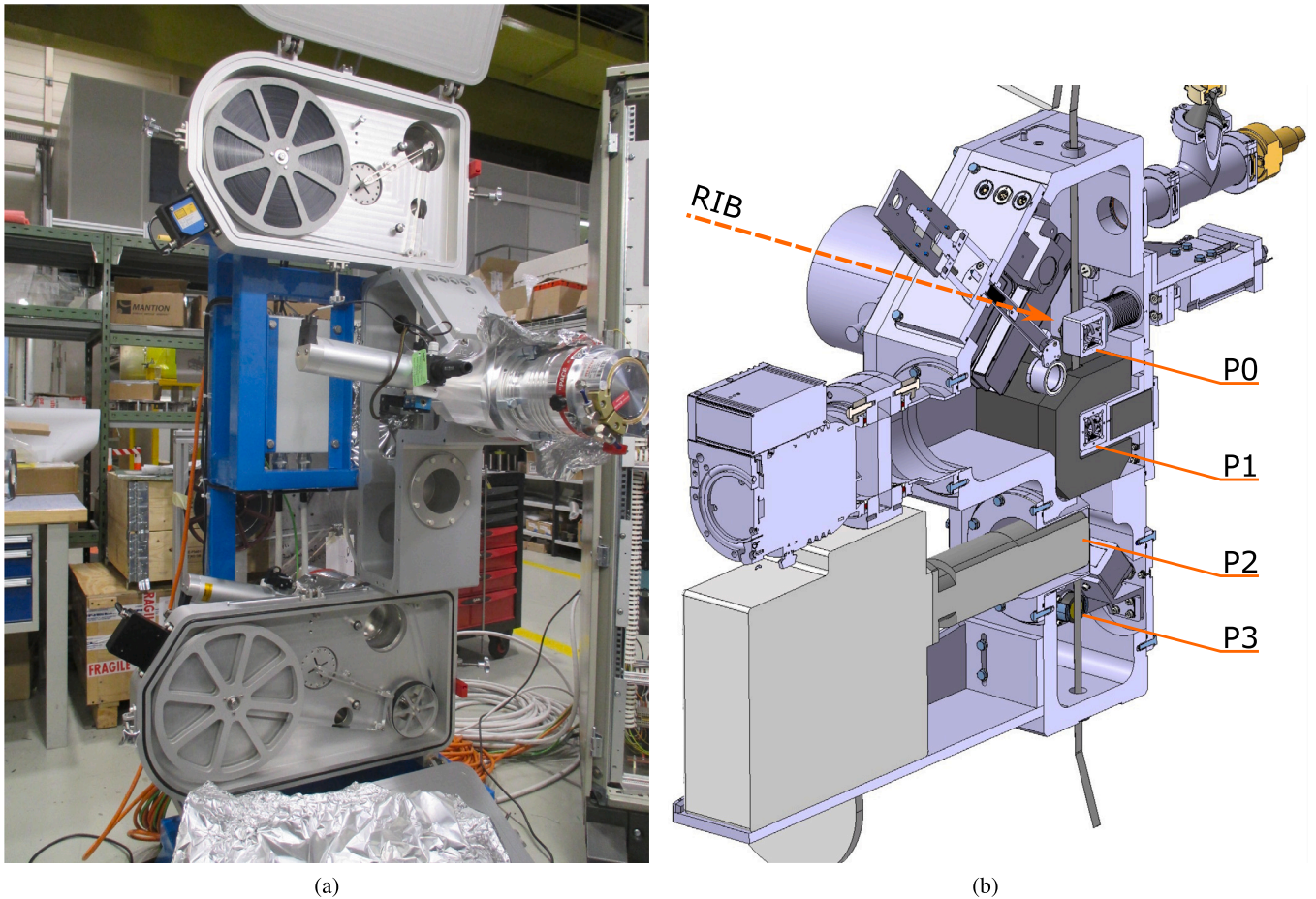


Fig. 1. (a) Picture of the fast tape station chassis with the reel and detector boxes open. (b) Schematic cross section of the detector box located between the upper and lower reel boxes. P0-P3 indicate the four detector positions.

When starting a measurement cycle, first, the tape is further strained by moving the upper tension arm via the two large bobbins. Once triggered, the capstan rapidly drives the tape, and the tension arm is released. Inductive positioning sensors (Pepperl+Fuchs PMI360D-F130-IE8-V15) monitor the tension arm's movement. In this way, the large reels that carry the majority of the heavy tape must only move in-between two measurement cycles such that slow motors would suffice. However, for simplicity and compatibility the same motors as described above are used for the reels. To monitor the remaining tape length, distance meters (SICK OD2-P120W6012) based on laser triangulation are installed in both tape boxes. Their position was chosen such that the light does not interfere with the radiation detectors.

2.2. The detector box

The detector box (Fig. 1(b)) is a machined aluminium case with ten ports. Two ports connect to the upper and lower tape boxes, one to the beam line (left and right), five are used for detectors and beam-instrumentation devices¹ and two are used for a vacuum pump and pressure gauges. The tape moves from upper to lower tape box and is horizontally displaced from the beam-line axis. The RIB, normally passing through the detector box and continuing in ISOLDE's central

beam line, can be deflected onto the tape by a set of electrostatic deflection plates. Starting from the implantation point, four detector positions (P0-P3) are vertically displaced. P0 accommodates a 2π in-beam β -detector, P1 a 4π β -detector, P2 a high-purity germanium (HPGe) γ -detector. P3 will accommodate an α -detector (Si-PIPS) and an additional β -detector, which will be located close to P2 to create β - γ coincidences (see Fig. 1(b)). Table 1 summarizes the detector positions and their respective distances from the implantation point. Compromising between speed and reliability, i.e. preventing tape slippage, transport times of 100 ms to any of the detector positions can be achieved. This is a 10-fold improvement compared to the previous tape station. All β -detectors are newly developed $23 \times 23 \times 3$ mm³ plastic scintillators (ELJEN EJ-200) coupled to a 3×3 Si-photomultiplier (SiPM) array based on MicroFJ-60035-TSV-TR1, J-Type 6×6 mm² cells from ONSEMI. An integrated front end electronics (FEE) preamplifier enhances the SiPM output signals within a compact $30 \times 30 \times 30$ mm³ aluminium casing. The dedicated FEE preamplifiers feature improved noise characteristics as the weak SiPM output signals are not passed through lengthy and noisy environment before amplification, as it was the case in the previous tape station. More detailed information about the β -detectors can be found in [3]. Fig. 1(b) schematically shows the detector positions. The in-beam β -detector is single-sided (2π) and equipped with a segmented collimator. The current of the individual collimator plates can be acquired independently, assisting initial beam tuning. The 4π β -detector consists of two detectors on each side of the tape, thereby nearly covering the full solid angle. Detection

¹ Adapted version of beam-instrumentation systems that are commonly employed at CERN.

Table 1

Detector positions located in the detector box of the fast tape station. The distance refers to the distance from the implantation point.

Position	Distance [mm]	Detector
P0	0	In-beam (2π) β -detector
P1	110	4π β -detector
P2	240	HPGe γ -detector
P3	330	2π α -detector ^a

^aWill be installed during Q2 2023.

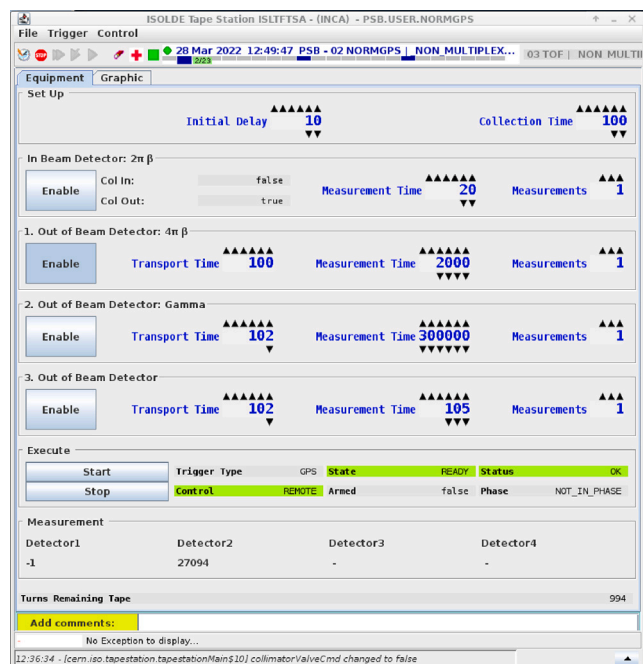


Fig. 2. FTS front end control application.

efficiencies of 90% were calculated from GEANT4 [4,5] simulations for β -energies greater 200 keV with a 100 keV threshold to cut signals originating from γ -rays. A 4 cm thick lead shielding reduces background radiation from long-lived activity present in the beam line and tape reels. The low background and high detection efficiency make this detector suitable for precision measurements and thus the primary asset for yield determination. Gamma-radiation is recorded using a coaxial HPGe-detector with a Cryo-Pulse 5-SL electronic cryostat (CANBERRA), featuring full widths at half maxima of 1.2 (2) keV at 120 (1300) keV photon energy, and 24 h cool-down time. The fast and slow output signals of all detectors are split. One set is passed to counters with associated analog modules. The second set enters a CAEN DT55725 digitizer, providing live data read-out.

2.3. Control system

Next to capable hardware, precision measurements of produced RIBs require an adequate control system. Most of the control hardware is based on Siemens components, which are widely used at CERN. On the PLC system, a real-time control code regulates all devices to move the tape and acquire data using the counters. To enable remote control and to synchronize measurement cycles to the pulsed proton beam delivery of CERN's accelerator complex, the control system takes advantages of the CERN-supported front end software architecture

(FESA) framework. Device control and communication is facilitated by means of FESA device classes, developed based on generalized and modular code that is adapted to the individual instruments. This framework transfers data from the user front end application and allows subscription to other device classes within the CERN network such that the timing signals provided by the proton accelerator complex can serve as triggers. While the FESA infrastructure cannot communicate directly with the PLC, this feature is realized utilizing the CERN-developed Software Infrastructure for Low-level Equipment ControllerS (SILECS) framework. Fig. 2 shows the front end application to configure and start a FTS measurement cycle. The user can specify the detector position, initial delay after proton impact, collection time, transport time², measurement time and the amount of subsequent measurements using the counters. All times are expressed in milliseconds. The bargraphic (top) indicates the subscription to the proton pulses' timing and destination data that is used as a trigger to start a measurement cycle. The dark blue colour corresponds to pulses which are delivered to ISOLDE. A complementary software tool was developed to launch a series of measurement cycles, differing in initial delay to determine the pulse shape, commonly denoted as release curve, of the produced RIB [6]. Such measurements are valuable and frequently performed at ISOLDE.

3. Summary

A new fast tape station was developed and integrated into ISOLDE's central beam line. Key improvements compared to the previous design are reduced transport times (100 ms) and improved β -detector noise characteristics. Since 2021, the device is routinely used for yield determination and quality control of produced radioactive ion beams.

Declaration of competing interest

The authors declare that they have no known competing financial interests or personal relationships that could have appeared to influence the work reported in this paper.

Acknowledgements

This project has received funding from the European's Union Horizon 2020 Research and Innovation Programme under grant agreement number 861198 project 'LISA' (Laser Ionization and Spectroscopy of Actinides) Marie Skłodowska-Curie Innovative Training Network (ITN). Further funding was received from the Romanian IFA Grant CERN/ISOLDE.

References

- [1] R. Catherall, W. Andreatza, M. Breitenfeldt, A. Dorsival, G.J. Focker, T.P. Gharsa, T.J. Giles, J.L. Grenard, F. Locci, P. Martins, S. Marzari, J. Schipper, A. Shornikov, T. Stora, J. Phys. G: Nucl. Part. Phys. 44 (9) (2017) <http://dx.doi.org/10.1088/1361-6471/aa7eba>.
- [2] J. Ballof, J.P. Ramos, A. Molander, K. Johnston, S. Rothe, T. Stora, C.E. Düllmann, Nucl. Instrum. Methods Phys. Res., Sect. B 463 (2020) 211–215, <http://dx.doi.org/10.1016/j.nimb.2019.05.044>.
- [3] C. Neacșu, R. Lică, G. Pascovici, C. Mihai, S. Rothe, Nucl. Instrum. Methods Phys. Res., Sect. A 1026 (2022) 166213, <http://dx.doi.org/10.1016/j.nima.2021.166213>.
- [4] S. Agostinelli, J. Allison, K. Amako, J. Apostolakis, H. Araujo, P. Arce, M. Asai, D. Axen, S. Banerjee, G. Barrand, F. Behner, L. Bellagamba, J. Boudreau, L. Broglia, A. Brunengo, H. Burkhardt, S. Chauvie, J. Chuma, R. Chytráček, G. Cooperman, G. Cosmo, P. Degtyarenko, A. Dell'Acqua, G. Depaola, D. Dietrich, R. Enami, A. Feliciello, C. Ferguson, H. Fesefeldt, G. Folger, F. Foppiano, A. Forti, S. Garelli, S. Giani, R. Giannitrapani, D. Gibin, J.J. Gomez Cadenas, I. Gonzalez, G. Gracia Abril, G. Greeniaus, W. Greiner, V. Grichine, A. Grossheim,

² Transport times of 100 ms are hard-coded on the PLC level to all detectors. Longer times are introduced as further delay after tape movement.

- S. Guatelli, P. Gumplinger, R. Hamatsu, K. Hashimoto, H. Hasui, A. Heikkinen, A. Howard, V. Ivanchenko, A. Johnson, F.W. Jones, J. Kallenbach, N. Kanaya, M. Kawabata, Y. Kawabata, M. Kawaguti, S. Kelner, P. Kent, A. Kimura, T. Kodama, R. Kokoulin, M. Kossov, H. Kurashige, E. Lamanna, T. Lampen, V. Lara, V. Lefebure, F. Lei, M. Liendl, W. Lockman, F. Longo, S. Magni, M. Maire, E. Medernach, K. Minamimoto, P. Mora de Freitas, Y. Morita, K. Murakami, M. Nagamatu, R. Nartallo, P. Nieminen, T. Nishimura, K. Ohtsubo, M. Okamura, S. O'Neale, Y. Oohata, K. Paech, J. Perl, A. Pfeiffer, M.G. Pia, F. Ranjard, A. Rybin, S. Sadilov, E. di Salvo, G. Santin, T. Sasaki, N. Savvas, Y. Sawada, S. Scherer, S. Sei, V. Sirotenko, D. Smith, N. Starkov, H. Stoecker, J. Sulkimo, M. Takahata, S. Tanaka, E. Tcherniaev, E. Safai Tehrani, M. Tropeano, P. Truscott, H. Uno, L. Urban, P. Urban, M. Verderi, A. Walkden, W. Wander, H. Weber, J.P. Wellisch, T. Wenaus, D.C. Williams, D. Wright, T. Yamada, H. Yoshida, D. Zschesche, GEANT4 - A simulation toolkit, *Nucl. Instrum. Methods Phys. Res., Sect. A* 506 (3) (2003) 250–303, [http://dx.doi.org/10.1016/S0168-9002\(03\)01368-8](http://dx.doi.org/10.1016/S0168-9002(03)01368-8).
- [5] J. Allison, K. Amako, J. Apostolakis, H. Araujo, P.A. Dubois, M. Asai, G. Barrand, R. Capra, S. Chauvie, R. Chytracek, G.A. Cirrone, G. Cooperman, G. Cosmo, G. Cuttone, G.G. Daquino, M. Donszelmann, M. Dressel, G. Folger, F. Foppiano, J. Generowicz, V. Grichine, S. Guatelli, P. Gumplinger, A. Heikkinen, I. Hrivnacova, A. Howard, S. Incerti, V. Ivanchenko, T. Johnson, F. Jones, T. Koi, R. Kokoulin, M. Kossov, H. Kurashige, V. Lara, S. Larsson, F. Lei, F. Longo, M. Maire, A. Mantero, B. Mascialino, I. McLaren, P.M. Lorenzo, K. Minamimoto, K. Murakami, P. Nieminen, L. Pandola, S. Parlati, L. Peralta, J. Perl, A. Pfeiffer, M.G. Pia, A. Ribon, P. Rodrigues, G. Russo, S. Sadilov, G. Santin, T. Sasaki, D. Smith, N. Starkov, S. Tanaka, E. Tcherniaev, B. Tomé, A. Trindade, P. Truscott, L. Urban, M. Verderi, A. Walkden, J.P. Wellisch, D.C. Williams, D. Wright, H. Yoshida, M. Peirgentili, Geant4 developments and applications, *IEEE Trans. Nucl. Sci.* 53 (1) (2006) 270–278, <http://dx.doi.org/10.1109/TNS.2006.869826>.
- [6] J. Lettry, R. Catherall, P. Drumm, P. Van Duppen, A.H. Evensen, G.J. Focker, A. Jokinen, O.C. Jonsson, E. Kugler, H. Ravn, *Nucl. Instrum. Methods Phys. Res., Sect. B* 126 (1–4) (1997) 130–134, [http://dx.doi.org/10.1016/S0168-583X\(96\)01025-7](http://dx.doi.org/10.1016/S0168-583X(96)01025-7).